67-kDa laminin receptor increases cGMP to induce cancer-selective apoptosis

Motofumi Kumazoe,[1] Kaori Sugihara,[1] Shuntaro Tsukamoto,[1] Yuhui Huang,[1]
Yukari Tsurudome,[1] Takashi Suzuki,[1] Yumi Suemasu,[1] Naoki Ueda,[1] Shuya Yamashita,[1]
Yoonhee Kim,[1] Koji Yamada,[1] and Hirofumi Tachibana[1,2]

[1]Division of Applied Biological Chemistry, Department of Bioscience and Biotechnology, Faculty of Agriculture, and
[2]Food Functional Design Research Center, Kyushu University, Fukuoka, Japan.

The 67-kDa laminin receptor (67LR) is a laminin-binding protein overexpressed in various types of cancer, including bile duct carcinoma, colorectal carcinoma, cervical cancer, and breast carcinoma. 67LR plays a vital role in growth and metastasis of tumor cells and resistance to chemotherapy. Here, we show that 67LR functions as a cancer-specific death receptor. In this cell death receptor pathway, cGMP initiated cancer-specific cell death by activating the PKCδ/acid sphingomyelinase (PKCδ/ASM) pathway. Furthermore, upregulation of cGMP was a rate-determining process of 67LR-dependent cell death induced by the green tea polyphenol (−)-epigallocatechin-3-O-gallate (EGCG), a natural ligand of 67LR. We found that phosphodiesterase 5 (PDE5), a negative regulator of cGMP, was abnormally expressed in multiple cancers and attenuated 67LR-mediated cell death. Vardenafil, a PDE5 inhibitor that is used to treat erectile dysfunction, significantly potentiated the EGCG-activated 67LR-dependent apoptosis without affecting normal cells and prolonged the survival time in a mouse xenograft model. These results suggest that PDE5 inhibitors could be used to elevate cGMP levels to induce 67LR-mediated, cancer-specific cell death.

Introduction

The concept underpinning molecular targeting involves strategies that strike precisely at specific and vital molecular targets in cancer cells (1–3), thereby providing the ideal approach to cancer treatment. The 67-kDa laminin receptor (67LR) has been shown to be overexpressed in various types of cancer (4–7). Pathological studies have shown that increased expression of 67LR is correlated with the histological severity of lesions and tumor progression (5–7). Cancer-overexpressed 67LR is involved in increased expression of cyclins A and B and cyclin-dependent kinases 1 and 2, and 67LR knockdown has been shown to significantly reduce tumor growth in a mouse model (8). Moreover, cancer-overexpressed 67LR has been shown to induce adhesion-mediated drug resistance (9), which indicates that 67LR has a vital role in cancer progression.

Polyphenol (−)-epigallocatechin-3-O-gallate (EGCG) inhibits the growth of tumor cells and induces apoptosis in cancer cells without adversely affecting normal cells (10–12), and several clinical trials have been carried out to evaluate its potential value as an anticancer agent (13–16). 67LR has been identified as a cell surface EGCG target that is essential for the antitumor effect of EGCG in vivo (17, 18). However, the mechanisms of the apoptotic pathway are incompletely understood. Furthermore, the plasma concentration of EGCG does not enable the killing of cancer cells. In the present study, we focused on the key mediator that determines 67LR-dependent apoptosis and used a molecular targeting strategy. Our results demonstrated that 67LR activated the peculiar apoptotic signaling Akt/eNOS/NO/cGMP/PKCδ pathway. Furthermore, we revealed that upregulation of cGMP could be a rate-determining process of 67LR-dependent cell death.

Phosphodiesterases (PDEs), major negative regulators of cGMP, act by degrading the phosphodiester bond. The characteristics of specific isoforms of PDEs regulating specific signaling pathways (19) are ideal drug targets, due to selective inhibition of specific PDE isoforms (20). PDE5 is one of the enzymes of PDEs and a major negative regulator of cGMP. PDE5 expression has been observed in corpus cavernosum, vascular smooth muscle cells, and platelets. Inhibition of PDE5 is an attractive approach for the relief of erectile disorders, because it enhances sexual arousal–induced cGMP signaling without severe side effects (21). However, little is known about the expression and role of PDE5 in cancer cells.

Here, we demonstrated that cancer-overexpressed PDE5, a negative regulator of cGMP, attenuated 67LR-dependent cell death induced by EGCG. A PDE5-selective inhibitor used for treating erectile dysfunction potentiated the anticancer effect of the 67LR activator in cancer cells, including breast, gastric, pancreatic, prostate, and multiple myeloma (MM) cancers. These results demonstrated that cGMP elevation caused by targeting the overexpressed 67LR and PDE5 in cancer cells may be a useful approach for cancer-specific chemotherapy.

Results

67LR-dependent NO production by Akt and eNOS activation is a key event in the EGCG-induced cell death pathway. 67LR has been shown to be involved in shear stress–induced eNOS expression in normal endothelial cells (22). Therefore, we investigated the role of NO in 67LR-dependent cell death. Primary MM cells derived from a MM patient, MM cell lines U266 and RPMI8226, and normal PBMCs were treated with EGCG (a natural ligand of 67LR) for 3 hours, and NO production was evaluated. EGCG induced NO production in MM cell lines and primary MM cells, but had no effect on PBMCs from healthy donors (Figure 1A). We also found that EGCG elicited eNOS phosphorylation at Ser1177, which is involved in eNOS activation (23), and that this phosphorylation was attenuated by pretreatment of MM cells with an anti-67LR monoclonal antibody (Figure 1B). These results suggested that EGCG activates eNOS
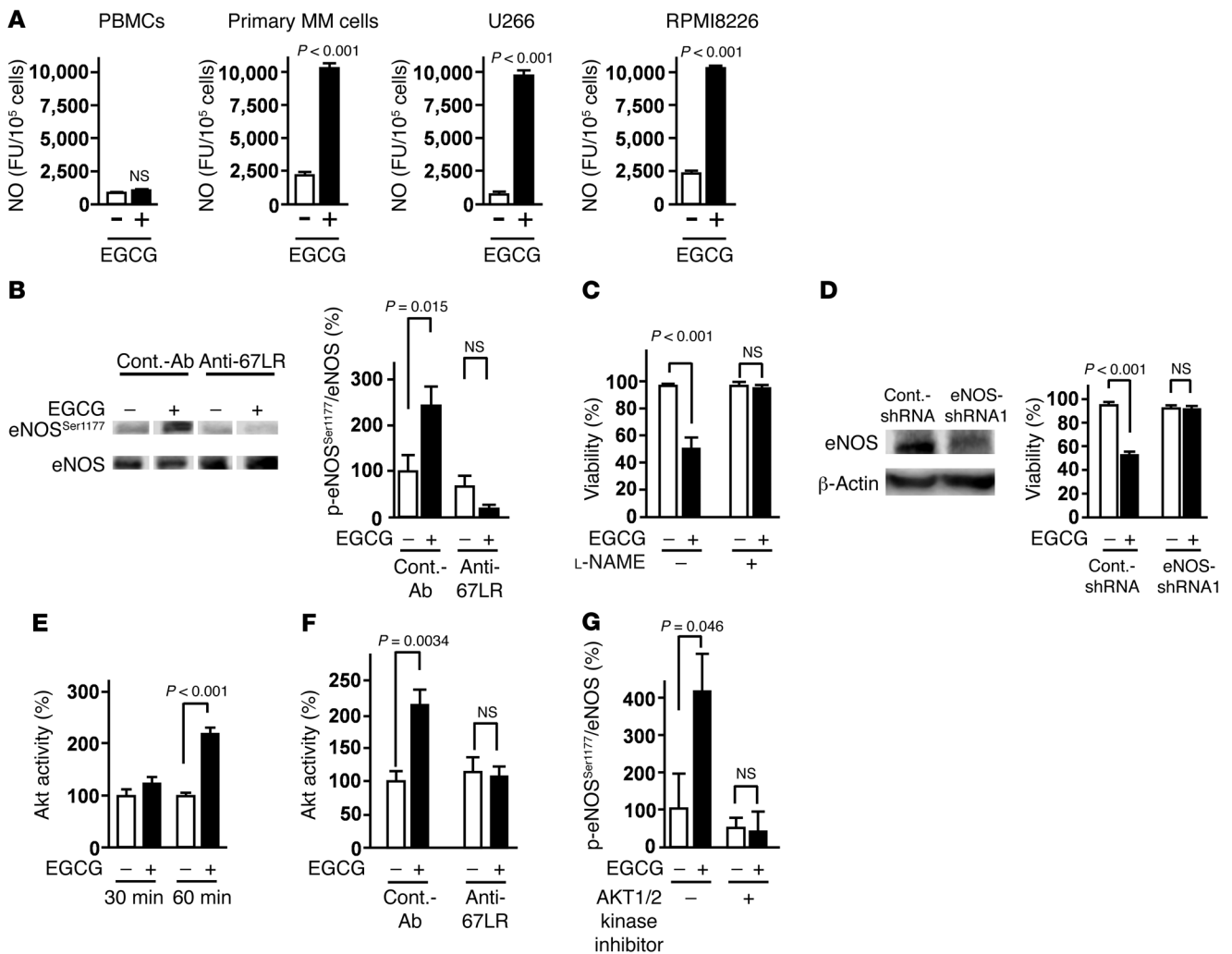
Figure 1

67LR-dependent NO production by activation of Akt and eNOS is a key event in the EGCG-induced cell death pathway. (**A**) Primary MM cells, MM cell lines (U266 and RPMI8226), and normal PBMCs were cultured for 3 hours in the absence or presence of 5 μM EGCG. NO production was measured using the fluorescent probe DAF-2DA. FU, fluorescence units. (**B**) Cells were pretreated with control antibody or anti-67LR antibody (20 μg/ml) and treated or not with EGCG for 3 hours. Phosphorylation of eNOS at Ser1177 was measured by Western blotting. Lanes were run on the same gel but were noncontiguous (white lines). (**C**) U266 cells were pretreated or not with the NOS inhibitor L-NAME (10 mM), then cultured in medium with or without 10 μM EGCG for 96 hours. (**D**) Left: Immunoblot analyses of eNOS knockdown in U266 cells. Right: Sensitivity of U266 cells to EGCG (10 μM for 96 hours) after eNOS knockdown. (**E**) Effect of 5 μM EGCG on Akt activity. (**F**) Cells were pretreated with control antibody or anti-67LR antibody (20 μg/ml) and treated or not with 5 μM EGCG for 1 hour. (**G**) U266 cells were pretreated or not with 5 μM AKT1/2 kinase inhibitor, then cultured in medium with or without 5 μM EGCG for 3 hours. All data are mean ± SEM.

and induces NO production via 67LR. To assess the role of NO in EGCG-induced cell death, we examined the effect of the NOS inhibitor L-NAME, which abrogated the cell death elicited by EGCG (Figure 1C). To confirm the involvement of eNOS in the anti-MM effect of EGCG, we transfected U266 cells with a lentivirus encoding scrambled control shRNA or shRNA against eNOS (Figure 1D and Supplemental Figure 1; supplemental material available online with this article; doi:10.1172/JCI64768DS1). Remarkably, silencing of eNOS abrogated the inhibitory effect of EGCG on cell viability. Akt (also referred to as PKB) is activated in endothelial cells in response to shear stress and mediates the activation of eNOS by phosphorylation at Ser1177, leading to an increase in NO production (23). Hence, we hypothesized that EGCG induces eNOS

activation through Akt. Our results demonstrated that EGCG increased Akt kinase activity (Figure 1E), which was attenuated by pretreatment of MM cells with an anti-67LR monoclonal antibody (Figure 1F). Importantly, an AKT1/2 kinase inhibitor attenuated EGCG-induced phosphorylation of eNOS at Ser1177 (Figure 1G). Taken together, our findings indicate that EGCG induces NO production through 67LR-dependent activation of Akt and eNOS.

67LR acts as a death receptor through cancer-specific cGMP upregulation. Next, we investigated the effect of EGCG on intracellular cGMP, a crucial mediator in NO-induced signaling (24). EGCG elevated the amount of cGMP in a dose-dependent manner in primary MM cells and U266 cells, but had no effect on normal PBMCs (Figure 2A and Supplemental Figure 2). To investigate whether cGMP acti-
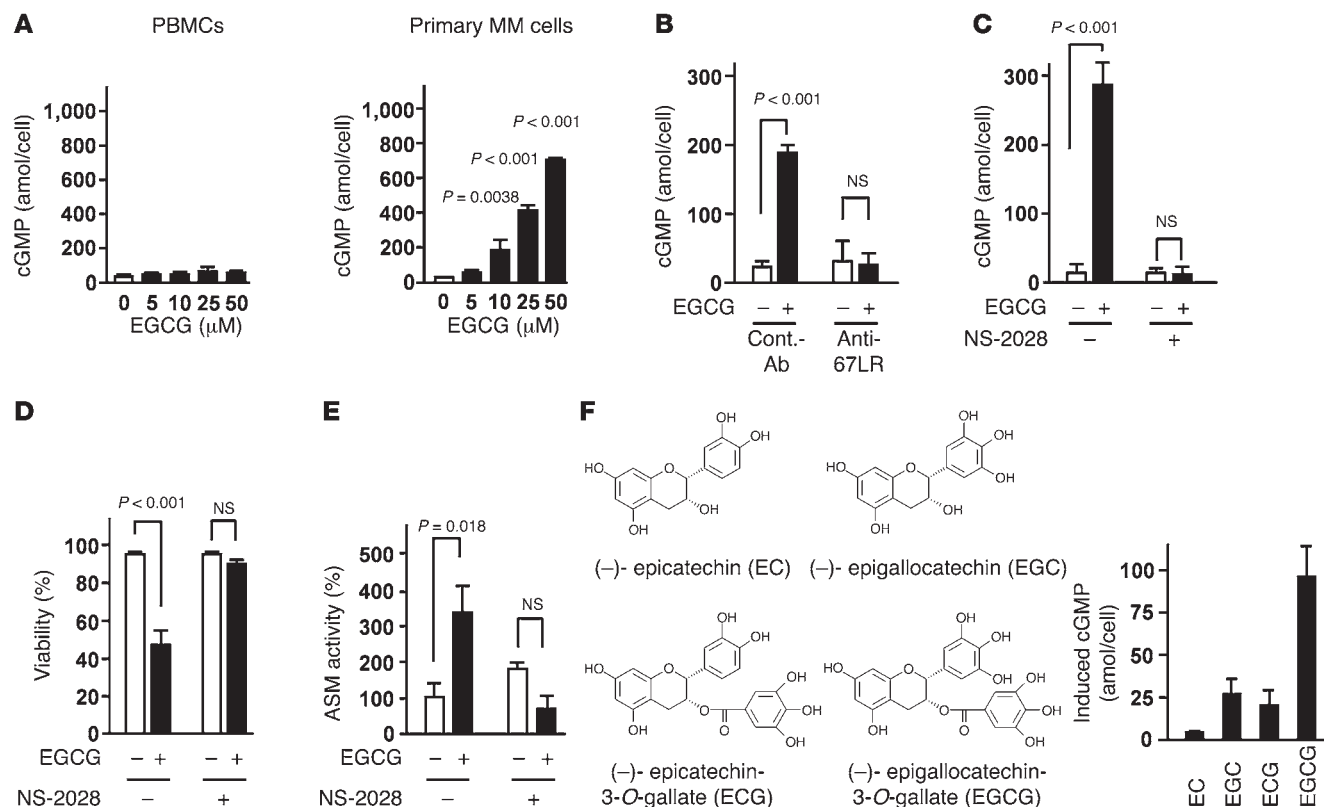
Figure 2

67LR acts as a death receptor via cancer-specific cGMP upregulation. (**A**) Effect of EGCG on cGMP levels in normal PBMCs and primary MM cells for 3 hours. (**B**) U266 cells were preincubated with anti-67LR antibody (20 μg/ml) or IgM control antibody (20 μg/ml), then treated or not with 10 μM EGCG for 3 hours. (**C**) Effect of the sGC inhibitor NS-2028 on cGMP upregulation. U266 cells were preincubated or not with 5 μM NS-2028 for 1 hour, then treated or not with 10 μM EGCG for 3 hours. (**D**) Effect of NS-2028 on cell death induced by EGCG. U266 cells were preincubated or not with 5 μM NS-2028 for 1 hour, then treated or not with 10 μM EGCG for 96 hours. (**E**) Effect of NS-2028 on EGCG-induced ASM activation, measured by TLC analyses. U266 cells were preincubated or not with 5 μM NS-2028 for 1 hour, then treated or not with 10 μM EGCG for 3 hours. (**F**) U266 cells were treated with 10 μM EGCG or its analogs for 3 hours, and cGMP levels in cells were measured using a competitive immunoassay. $n = 3$ per group. All data are mean ± SEM.

vates the 67LR-dependent apoptotic pathway, we examined the effects of the cell-permeable cGMP analog dibutyryl-cGMP on the activation of acid sphingomyelinase (ASM), which plays an indispensable part in EGCG-induced cell death (Supplemental Figure 3 and ref. 25). Our data showed that dibutyryl-cGMP induced ASM activation in a dose-dependent manner (Supplemental Figure 4). Pretreatment of U266 cells with anti-67LR antibody inhibited EGCG-induced cGMP elevation (Figure 2B). NO increased the intercellular cGMP level by activating soluble guanylate cyclase (sGC). The sGC inhibitor NS-2028 prevented the cGMP upregulation induced by EGCG (Figure 2C). Furthermore, NS-2028 pretreatment also attenuated EGCG-induced cell death and ASM activation (Figure 2, D and E). Taken together, these results suggested that the 67LR/Akt/eNOS/NO/sGC/cGMP pathway mediates EGCG-induced cell death. Other tea catechins and their structurally related compounds have little affinity for 67LR (17) and did not affect the intracellular cGMP level (Figure 2F).

Abnormal overexpression of PDE5 attenuates EGCG-induced cell death in MM cells. Our findings revealed that cGMP has a crucial role in EGCG-induced MM-specific cell death. EGCG inhibited U266 cell growth with an IC_{50} of 23.2 μM (Supplemental Figure 8A). This concentration was much higher than the plasma concentration

previously observed in clinical trials (13). EGCG at physiologically achievable levels could induce NO production (Figure 1A), but could not upregulate the level of cGMP sufficiently to induce MM cell death (Supplemental Figure 2). These results suggested that upregulation of cGMP may be a "choke point" of the EGCG-induced apoptotic signaling pathway. PDEs are enzymes that inactivate cGMP signaling by hydrolyzing the 3′,5′-phosphodiester bond. We hypothesized that the PDEs may protect MM cells from EGCG-induced cell death by downregulating the cGMP level. To determine the effect of various PDEs on the anti-MM effect of EGCG, myeloid cell lines were pretreated with inhibitors of different PDEs (Figure 3, A and B). Significant inhibition of cell proliferation was observed when EGCG was combined with the PDE5-selective inhibitors zaprinast, methoxyquinazoline (MQZ), sildenafil, and vardenafil. PDE5 is one of the major negative regulators of cGMP signaling. However, the expression of PDE5 in MM cells is not known. The protein levels of PDE5 and 67LR increased substantially in the MM cells of 10 patients as well as all human MM cell lines compared with those in normal PBMCs of 10 healthy donors (Figure 3C). Surprisingly, a significant correlation was observed between expression of 67LR and PDE5 ($R_s = 0.895$, $P < 0.01$, Spearman rank test, $n = 14$; Figure 3C, right blot, and Supplemental
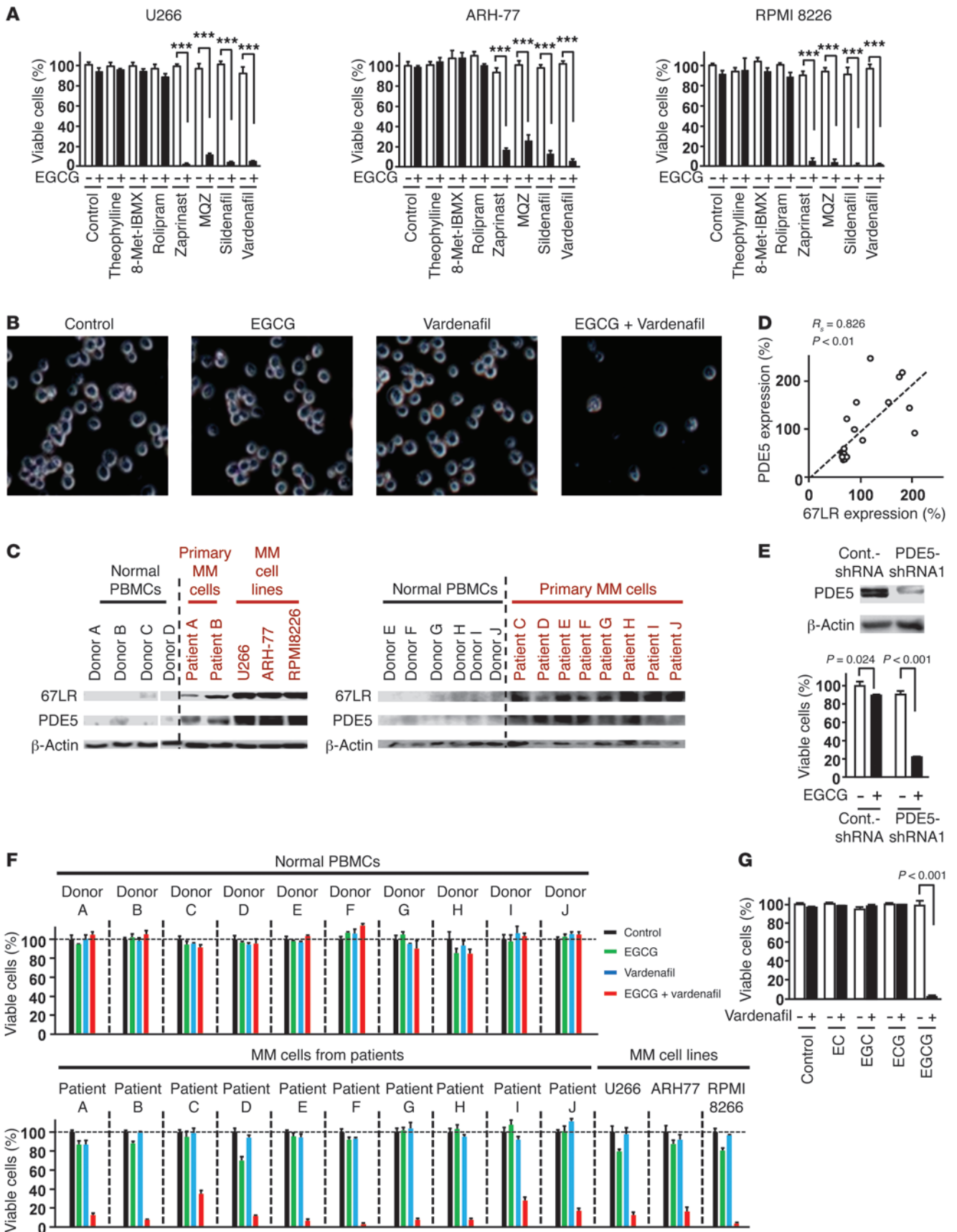
Figure 3

Abnormal overexpression of PDE5 attenuates EGCG-induced cell death in MM cells. (**A**) MM cells were pretreated with the PDE1 inhibitor 8-Met-IBMX (20 μM), with the PDE4 inhibitor rolipram (10 μM), with the PDE5 inhibitors zaprinast (10 μM), sildenafil (10 μM), vardenafil (5 μM), and MQZ (10 μM), or with theophylline (20 μM), then treated or not with 5 μM EGCG for 96 hours. ***$P < 0.001$. (**B**) Cells were treated with or without 5 μM vardenafil and/or 5 μM EGCG for 96 hours. Phase-contrast images were taken by optical microscopy. Original magnification, ×20. (**C**) Expression of 67LR and PDE5 proteins in patient cells and normal PBMCs, assessed by immunoblotting. Lanes were run on the same gel but were noncontiguous (white lines). (**D**) Correlation between 67LR expression and PDE5 expression. (**E**) Top: Immunoblot analyses of PDE5 in U266 cells. Bottom: EGCG sensitivity (5 μM for 96 hours) of U266 cells after PDE5 knockdown. (**F**) Normal PBMCs from 10 healthy donors, primary MM cells from 10 patients, and MM cell lines were treated with or without 5 μM vardenafil and/or 5 μM EGCG for 96 hours. (**G**) U266 cells were incubated for 96 hours with or without 5 μM vardenafil and/or 5 μM EGCG analogs (see Figure 2F). $n = 3$ per group. All data are mean ± SEM.

Figure 5). In addition, we found a significant correlation between expression of 67LR and PDE5 in 10 MM tissues from 10 MM patients and 10 normal bone marrow tissues from 10 donors ($R_s = 0.826$, $P < 0.01$, Spearman rank test, $n = 20$; Figure 3D and Supplemental Figure 6). These data may provide a rational explanation for the insensitivity of MM cells to low concentrations of EGCG despite the high expression of 67LR. To confirm the role of PDE5 in EGCG resistance, we investigated the effect of PDE5 silencing. Western blot analysis indicated that transfection of PDE5 shRNA expression vector silenced PDE5 protein expression in this cell line without affecting the expression level of 67LR (Supplemental Figure 7). This reduction in the PDE5 protein expression markedly potentiated the anti-MM effect of EGCG (Figure 3E and Supplemental Figure 7). Furthermore, we showed that the PDE5 inhibitor vardenafil, which is used for treating erectile dysfunction (21), had no effect on the number of viable normal PBMCs from healthy donors, but significantly enhanced the killing activity of EGCG on primary MM cells from patients and from the MM cell lines U266, RPMI8226, and ARH-77 (Figure 3, A and F). Treatment with EGCG and vardenafil in combination resulted in greater inhibition of the growth of U266 cells, with an IC_{50} of 1.4 μM compared with 23.2 μM for EGCG alone (Supplemental Figure 8, A and B). Isobologram analyses showed that the growth-inhibitory effects of combined treatment with EGCG and vardenafil on the growth of U266 cells and RPMI8226 cells were synergistic (Supplemental Figures 8 and 9). We also found that vardenafil sensitized U266 cells to an EGCG derivative, epigallocatechin-3-O-(3-O-methyl)-gallate (EGCG 3″Me; Supplemental Figure 10), which has been known to enhance pharmacokinetic characteristics compared with EGCG. Conversely, vardenafil in combination with the other catechins did not induce cell death in MM cells (Figure 3G).

Effect of EGCG and vardenafil in combination on myeloma cell proliferation in vivo. EGCG and vardenafil in combination prevented cell proliferation more efficiently than did the conventional anti-MM drug lenalidomide in U266 cells in vitro (Figure 4A). The combination also inhibited the cell growth of the mouse myeloma cell line MPC-11 in vitro (Figure 4B). To evaluate the in vivo activity of EGCG and vardenafil in combination, female BALB/c mice (5 per group) were inoculated subcutaneously in the interscapular area with 5×10^6 MPC-11 cells in 100 μl RPMI 1640 medium; after the

appearance of palpable tumors, mice were then given a single i.p. injection of 15 mg/kg EGCG and/or 5 mg/kg vardenafil dissolved in physiological saline (0.9%). After 6 hours, tumors were excised to evaluate the effect on the activity of PKCδ and ASM, which have essential roles in EGCG-induced cell death (25). Injection i.p. of EGCG and vardenafil in combination increased PKCδ phosphorylation at Ser662 (corresponding to human p-PKCδ[Ser664]) as well as ASM activity (Figure 4, C and D). Moreover, this combination significantly upregulated the cleavage of caspase-3 (Figure 4E), a key mediator of apoptosis in tumor cells. Collectively, these results suggested that vardenafil potentiates the anticancer effect of EGCG through amplification of the downstream effectors PKCδ and ASM. To evaluate the long-term effect of EGCG and vardenafil in combination on tumor growth, female BALB/c mice (10 per group) were given i.p. injection of 15 mg/kg EGCG and/or 5 mg/kg vardenafil every 2 days. The combination of EGCG and vardenafil significantly suppressed tumor growth in the mice (Figure 4F). Furthermore, log-rank analyses of the Kaplan-Meier survival curves showed a significant increase in the survival of mice treated with EGCG and vardenafil in combination compared with mice treated with saline, EGCG alone, or vardenafil alone (Figure 4G). To confirm whether PDE5 protects MM cells from EGCG-induced cell death in vivo, BALB/c mice were inoculated subcutaneously in the interscapular area with 5×10^6 MPC-11 cells stably transfected with control shRNA or the PDE5 shRNA expression vector; after the appearance of palpable tumors, mice were then given i.p. injection of 15 mg/kg EGCG every 2 days. A reduction in the expression of PDE5 protein markedly potentiated the anti-MM effect of EGCG in vivo (Supplemental Figure 11).

Mitochondrial transmembrane potential collapse and caspase activation are involved in 67LR-dependent cell death. To ascertain whether the combination of EGCG and vardenafil induces apoptosis, cells treated with this combination were stained sequentially with annexin V–Alexa Fluor 488 and observed by fluorescence microscopy and flow cytometry (Figure 5, A–C). The combination caused a significant reduction in the viability of U266 cells, with less than 10% of the cells being viable — i.e., negative for both annexin V and propidium iodide (PI) — after 96 hours of treatment. We then investigated the apoptotic pathway elicited by EGCG and vardenafil. Flow cytometric analyses showed an increase in the level of active caspase and in the collapse of mitochondrial transmembrane potential (Δφm) in cells treated with EGCG and vardenafil in combination (Figure 5, D and E). These results strongly suggested that EGCG and vardenafil in combination cause a pronounced induction of apoptosis in MM cells. To confirm the apoptosis-inducing effect of EGCG and vardenafil in combination, we undertook flow cytometric analyses of PI staining for cellular DNA content. The combination was observed to increase the population of U266 cells in the sub-G1 fraction (Figure 5F).

Inhibition of PDE5 potentiates 67LR-dependent cell death by enhancing the 67LR-dependent signaling pathway in MM cells. To determine whether the combination of EGCG and vardenafil induces 67LR-dependent cell death, we undertook antibody-blocking experiments, which demonstrated that 67LR mediated the apoptosis-inducing effect of this combination (Figure 6A). We also found that vardenafil potentiated EGCG-induced upregulation of cGMP in MM cells and enhanced the anti-MM effect of the sGC activator BAY 41-2272 (Figure 6, B and C). In addition, the ASM inhibitor desipramine abrogated the anti-MM effect of EGCG and vardenafil in combination (Figure 6D). To confirm the role of ASM in the anticancer
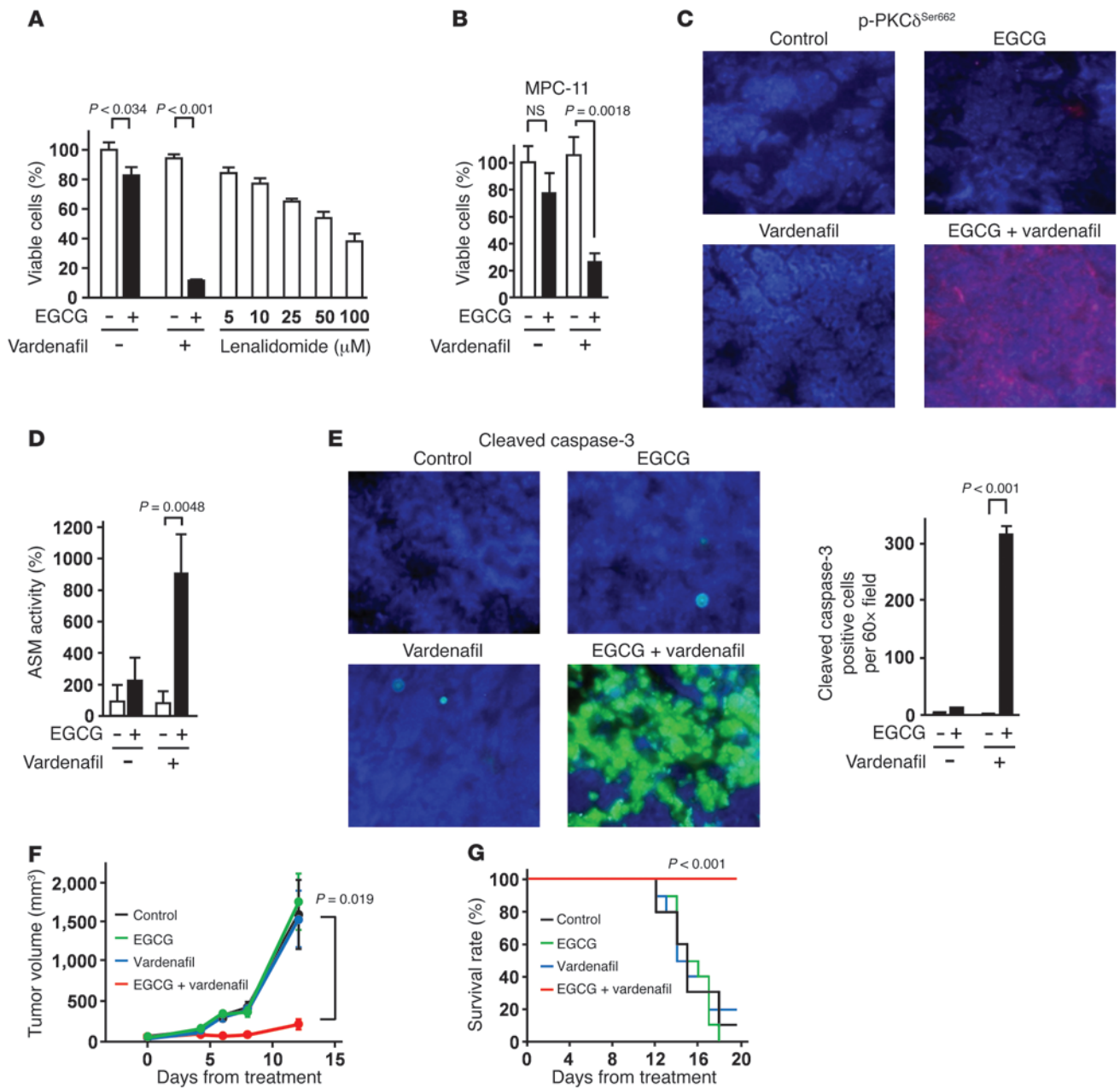
Figure 4

Effect of EGCG and a PDE5 inhibitor in combination on myeloma cell proliferation in vivo. (**A**) Anti-MM effect of EGCG (5 μM) and vardenafil (5 μM) in combination and of lenalidomide for 96 hours in vitro (*n* = 3). (**B**) Mouse myeloma MPC-11 cells were pretreated or not with 5 μM vardenafil for 3 hours and cultured in the presence or absence of 5 μM EGCG for 96 hours (*n* = 3). (**C–E**) MPC-11 cells were injected subcutaneously into female BALB/c mice, and mice (*n* = 5 per group) were given single i.p. injections of EGCG (15 mg/kg) and/or vardenafil (5 mg/kg). (**C**) After 6 hours, tumors were excised and evaluated for phosphorylation of PKCδ at Ser662 (corresponding to human p-PKCδ^{Ser664}). Original magnification, ×60. (**D**) ASM activation, assessed by TLC analyses. (**E**) Cleaved caspase-3 was evaluated by immunofluorescence analyses. Original magnification, ×60. (**F** and **G**) MPC-11 cells were injected subcutaneously into female BALB/c mice, and mice (*n* = 10 per group) were given i.p. injections of EGCG (15 mg/kg) and/or vardenafil (5 mg/kg) every 2 days. Statistical analyses of survival curves were undertaken using log-rank analyses of the Kaplan-Meier curves. All data are mean ± SEM.

effect of EGCG and vardenafil in combination, we transfected U266 myeloma cells with a lentivirus encoding scrambled control shRNA or shRNA against ASM. Remarkably, silencing of ASM abrogated the inhibitory effect of the combination on U266 cells (Figure 6E). Collectively, these results demonstrated that the PDE5 inhibitor

potentiated EGCG-induced apoptosis by enhancing the 67LR/cGMP/ASM-dependent signaling pathway in MM cells (Figure 6F).

PDE5 is overexpressed in various types of human cancer, and PDE5 inhibition potentiates the anticancer effect of EGCG. Next, we investigated the effect of EGCG and vardenafil in various types of cancer. The combi-
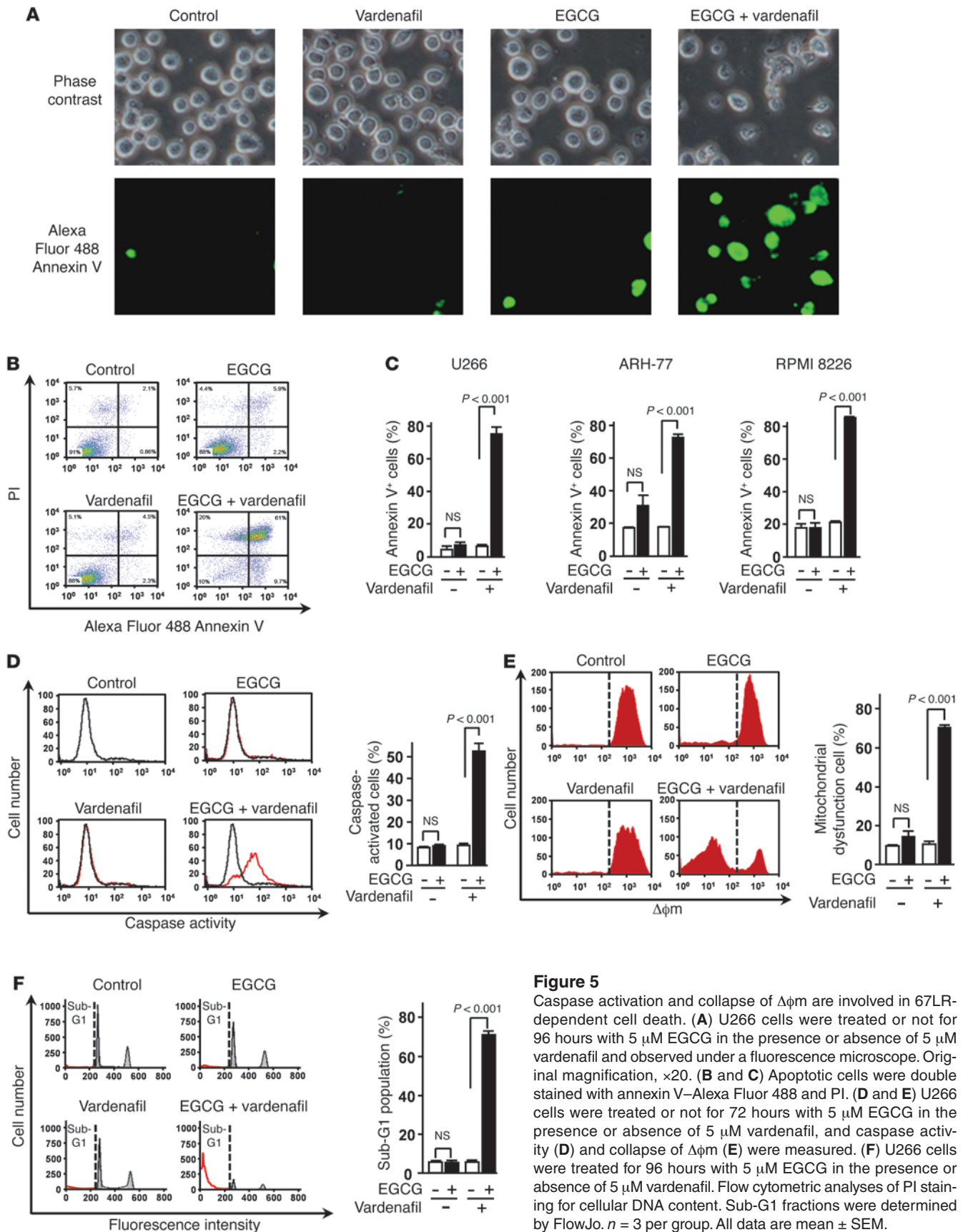
Figure 5

Caspase activation and collapse of $\Delta\phi$m are involved in 67LR-dependent cell death. (**A**) U266 cells were treated or not for 96 hours with 5 μM EGCG in the presence or absence of 5 μM vardenafil and observed under a fluorescence microscope. Original magnification, ×20. (**B** and **C**) Apoptotic cells were double stained with annexin V–Alexa Fluor 488 and PI. (**D** and **E**) U266 cells were treated or not for 72 hours with 5 μM EGCG in the presence or absence of 5 μM vardenafil, and caspase activity (**D**) and collapse of $\Delta\phi$m (**E**) were measured. (**F**) U266 cells were treated for 96 hours with 5 μM EGCG in the presence or absence of 5 μM vardenafil. Flow cytometric analyses of PI staining for cellular DNA content. Sub-G1 fractions were determined by FlowJo. $n = 3$ per group. All data are mean ± SEM.
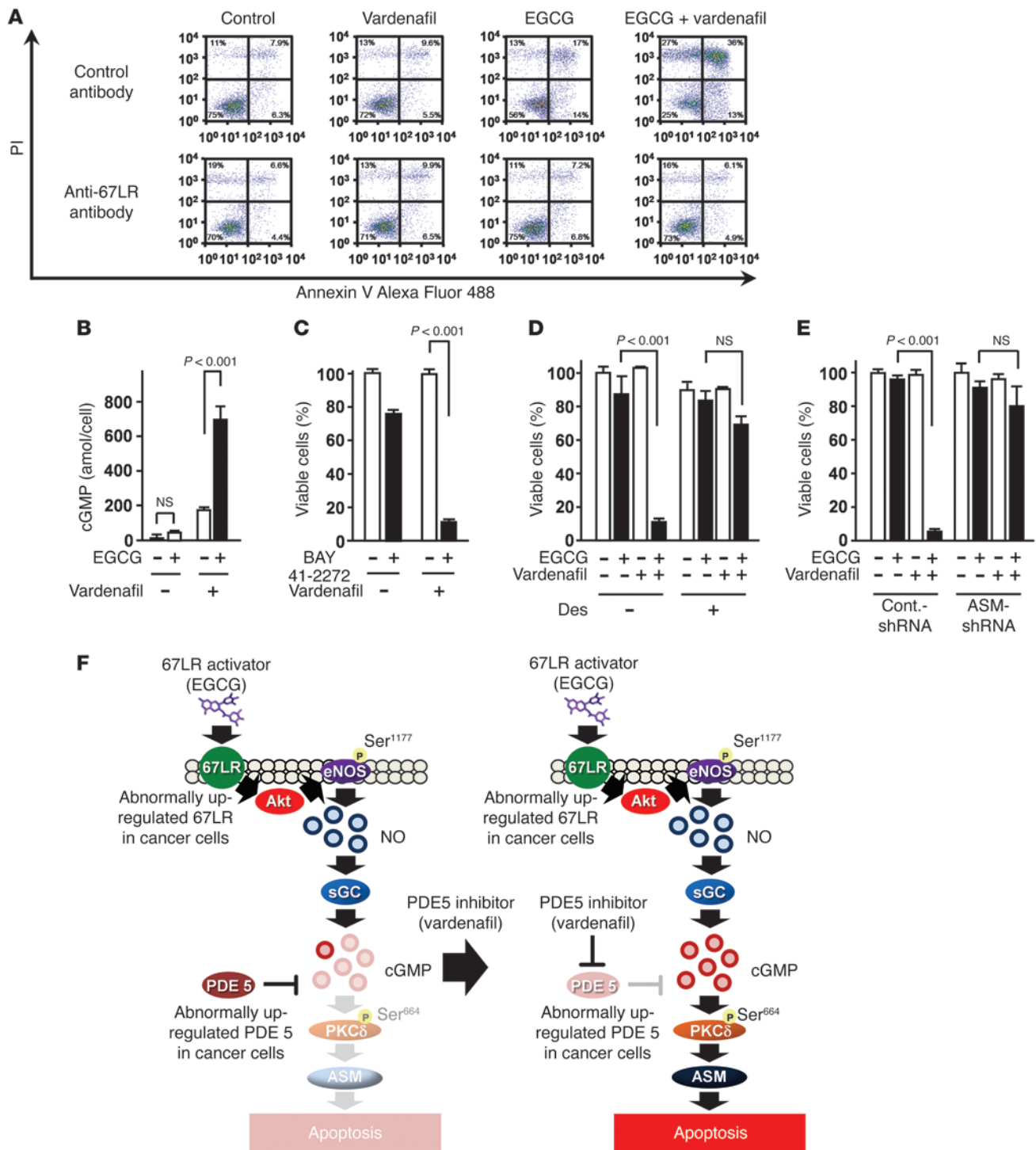
Figure 6

Inhibition of PDE5 potentiates 67LR-dependent cell death by enhancing the 67LR-dependent signaling pathway in MM cells. (**A**) U266 cells were preincubated for 3 hours with anti-67LR antibody or IgM control antibody, then treated or not for 96 hours with 5 μM EGCG and/or vardenafil. Apoptotic cells were double stained with annexin V–Alexa Fluor 488 and PI and analyzed by flow cytometry. (**B**) Cells were pretreated or not with 5 μM vardenafil and cultured for 3 hours in the presence or absence of 5 μM EGCG, followed by measurement of the amount of cGMP in the cells. (**C**) U266 cells were treated or not for 96 hours with the sGC activator BAY 41-2272 (1 μM) in the presence or absence of 5 μM vardenafil. (**D**) U266 cells were preincubated or not for 3 hours with the ASM-specific inhibitor desipramine (Des; 5 μM), then treated or not for 96 hours with 5 μM EGCG and/or vardenafil. (**E**) Sensitivity of U266 cells to EGCG and/or vardenafil (5 μM for 96 hours) after ASM knockdown. $n = 3$ per group. All data are mean ± SEM. (**F**) The combination of EGCG as a cancer-specific cGMP inducer with an inhibitor targeting cancer-overexpressed PDE5 could be a useful strategy for cancer-selective chemotherapy. Left: In the absence of PDE5 inhibitor, overexpressed PDE5 in cancer attenuates the anticancer effect of EGCG. Right: PDE5 inhibition potentiates the anticancer effect of EGCG.
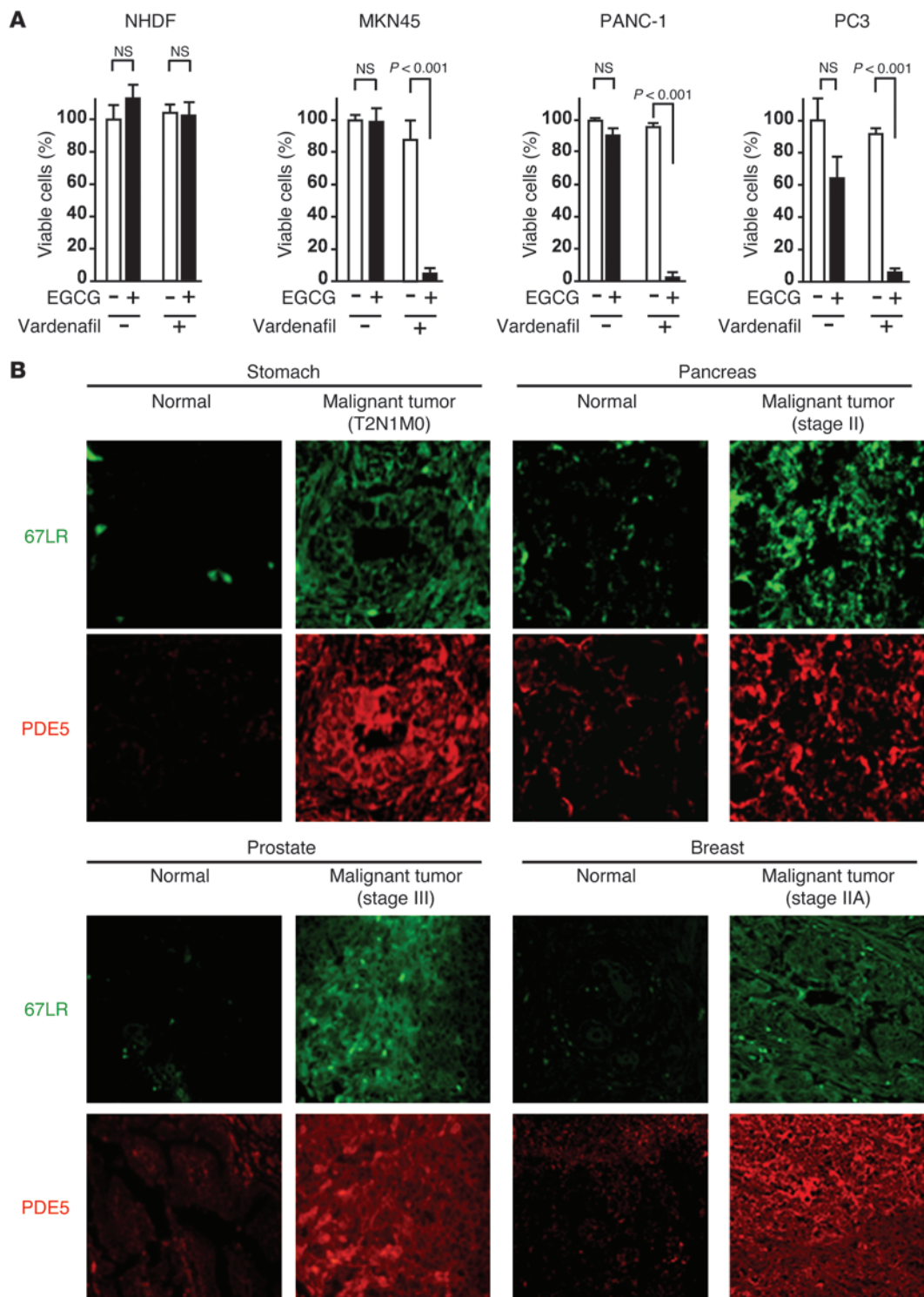
Figure 7
PDE5 is overexpressed in various types of human cancer. (**A**) NHDFs from healthy donors as well as cell lines MKN45 (gastric cancer), PANC-1 (pancreatic cancer), and PC3 (prostate cancer) were cultured for 96 hours with 5 μM vardenafil and/or 5 μM EGCG. (**B**) Representative images of paraffin sections of various types of tissue from cancer patients. Original magnification, ×60. n = 3 per group for all in vitro studies. All data are mean ± SEM.
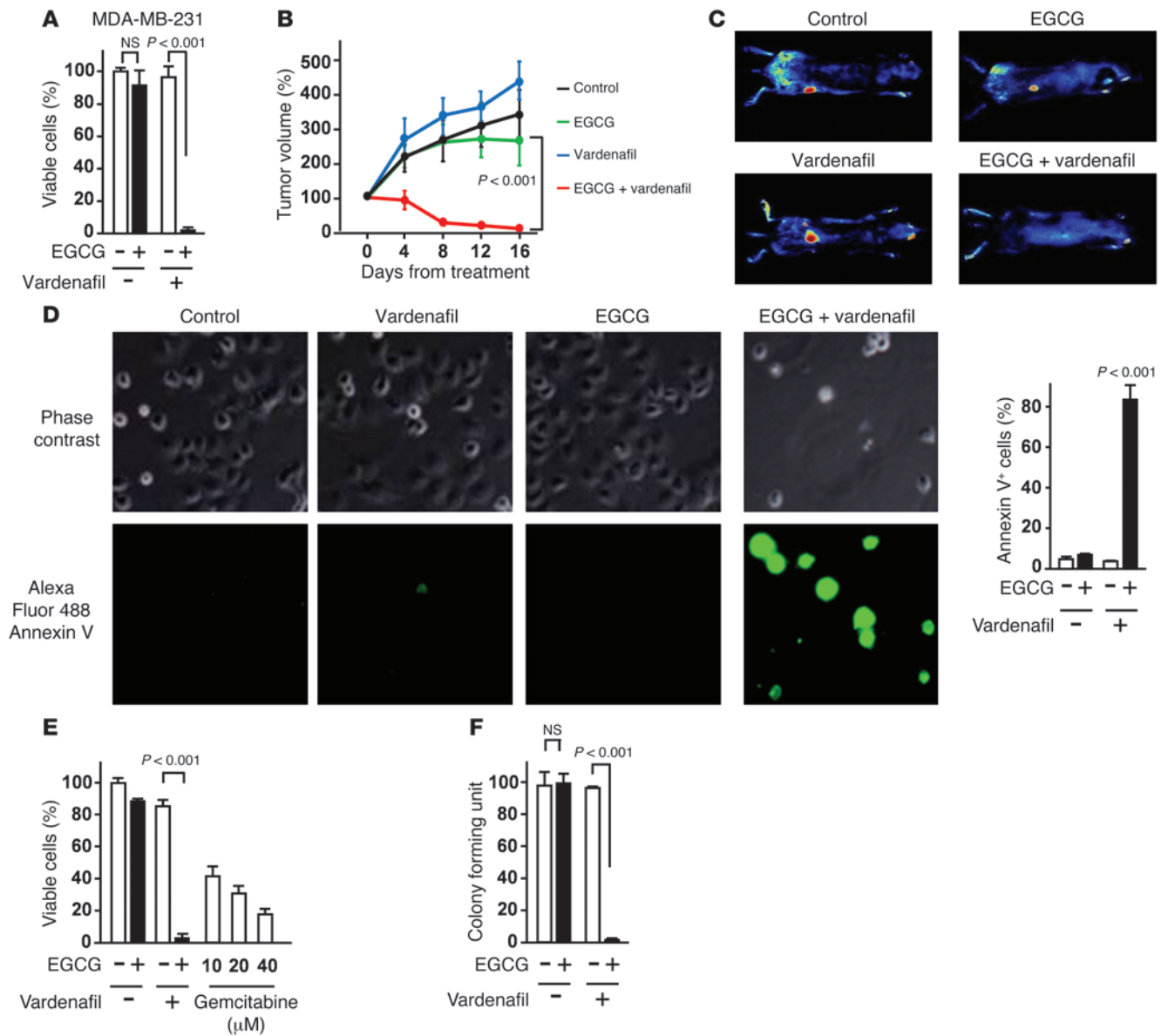
Figure 8
PDE5 inhibition potentiates the anticancer effect of EGCG. (**A**) MDA-MB-231-RFP cells were cultured for 96 hours with 5 μM vardenafil and/or 5 μM EGCG. (**B** and **C**) MDA-MB-231-RFP cells were injected subcutaneously into female nude mice, and mice (n = 8 per group) were given EGCG (15 mg/kg i.p.) and/or vardenafil (5 mg/kg i.p.). (**D**) PANC-1 cells were treated for 96 hours with 5 μM EGCG and/or 5 μM vardenafil. Cells were treated with annexin V–Alexa Fluor 488. Original magnification, ×20. (**E**) PANC-1 cells were treated with 5 μM EGCG and/or 5 μM vardenafil or with the conventional drug gemcitabine for 96 hours. (**F**) Clonogenic assay in PANC-1 cells. 1,500 PANC-1 cells were cultured for 10 days with 5 μM vardenafil in the presence or absence of 5 μM EGCG. n = 3 per group for all in vitro studies. All data are mean ± SEM.

nation of EGCG and vardenafil inhibited the proliferation of the gastric cancer cell line MKN45, the pancreatic cancer cell line PANC-1, and the prostate cancer cell line PC3, but did not affect normal human diploid fibroblasts (NHDFs) or normal HUVECs (Figure 7A and Supplemental Figure 12). Immunohistochemical analyses of paraffin-embedded tissue sections showed that levels of 67LR and PDE5 were elevated in various types of human cancers (gastric, pancreatic, prostate, and breast) compared with their normal counterparts (Figure 7B). The combination of EGCG and vardenafil inhibited proliferation of the human breast cancer cell line MDA-MB-231-RFP in vitro (Figure 8A). To evaluate the in vivo activity of

EGCG and vardenafil in combination on MDA-MB-231 cells, the cells were injected subcutaneously into female nude mice; after the appearance of palpable tumors, mice were given i.p. injections of 15 mg/kg EGCG and/or 5 mg/kg vardenafil every 2 days. EGCG and vardenafil in combination significantly suppressed tumor growth (Figure 8, B and C), and did not increase serum levels of ALT/AST (Supplemental Figure 13). In addition, the combination induced apoptosis in the pancreatic cancer cell line PANC-1 (Figure 8D). Furthermore, the effect of this combination was comparable with that of gemcitabine, a conventional anticancer drug used widely for treating pancreatic cancer (Figure 8E). A prior study showed that a PANC-1

cell subpopulation propagates colony formation and has the properties of stem cells (26). The combination of EGCG and vardenafil treatment inhibited colony formation in PANC-1 cells (Figure 8F).

Discussion

The present study addressed the novel cell death pathway mediated by the cancer-overexpressed 67LR. Here, we clarified that Akt/eNOS/NO/sGC/cGMP/PKCδ/ASM signaling elicited by EGCG bound to 67LR is a crucial step for this cell death pathway. 67LR-dependent eNOS activation and NO production played an indispensable part in EGCG-induced cell death. One study reported that phosphorylation of eNOS at Ser1177 is induced by the adenosine A_{2B} receptor (27) and acetylcholine receptor via a PI3K/Akt-dependent signaling pathway. We here identified 67LR as a cell surface receptor mediating eNOS activation in MM cells.

cGMP is one of the secondary messengers involved in the regulation of vascular homeostasis. Regulation of cGMP is a well-established strategy for vasodilatation and increased blood flow. To our knowledge, this is the first study to demonstrate that cGMP initiates an apoptotic pathway by activating the PKCδ/ASM pathway.

Activation of the PKCδ/ASM pathway is involved in downstream effectors in EGCG-induced apoptosis (25). These events (activation of PKCδ, ASM, and caspase-3) are well-known mechanisms involved in various pathways of apoptosis induced by oxidation stress, cisplatin, and ultraviolet light. However, in the present study, we revealed the characteristic mechanisms by which cancer-overexpressed 67LR acts as a novel death receptor. A prior study reported that PKCδ is one of the novel PKCs activated by diacylglycerol or 12-O-tetradecanoylphorbol 13-acetate (28), but is unresponsive to Ca^{2+}. It has also been reported that PKCδ activation is induced by oxidative stress (29), etoposide (30), ionizing radiation (31), and Fas (32). We demonstrated here that cGMP is a critical signal mediator in 67LR-dependent PKCδ/ASM activation and MM cell death. In addition, the NO-independent sGC activator BAY 41-2272 increased the phosphorylation level of PKCδ at Ser664, a surrogate marker for PKCδ activation (M. Kumazoe, unpublished observation). This molecular mechanisms involved in cGMP-induced PKCδ activation are not entirely clear. This issue is worthy of particular consideration to clarify the 67LR-dependent apoptotic pathway.

67LR is a nonintegrin cell surface receptor for laminin. It has vital roles in the metastasis and invasion of tumors as well as drug resistance (9). Several clinical studies have shown that overexpression of 67LR correlates with tumor progression (5–7). 67LR has been reported to have an indispensable role in tumor growth in a mouse model (8). However, our findings suggested that 67LR acts as a cancer-specific death receptor mediating the apoptotic signaling pathway. This finding suggested that 67LR may be an ideal novel target for cancer chemotherapy and may provide a rationale for the clinical effectiveness of EGCG as a 67LR-targeting drug.

EGCG alone has cytotoxic effects on MM cells only if applied at concentrations greater than 20 μM, considerably greater than the concentrations typically used in clinical trials. Combined treatment for targeting key resistant factors could be a useful strategy for overcoming drug resistance (33–35). Effective regimens have been developed to overcome resistance to anticancer drugs, such as gemcitabine/erlotinib in combination with an additional anticancer drug.

PDEs are major negative regulators of cGMP and act by degrading the phosphodiester bond. PDE5 is one of the enzymes of PDEs and a major negative regulator of cGMP. Its expression has been observed in corpus cavernosum, vascular smooth muscle cells, and platelets. However, little is known about the expression and role of PDE5 in cancer cells. Here, we demonstrated that PDE5, as a negative regulator of EGCG-induced apoptosis, was significantly overexpressed in various types of cancer, including MM and gastric, prostate, pancreatic, and breast cancers. We also showed that the PDE5 inhibitor vardenafil, which is used for the treatment of erectile dysfunction, dramatically potentiated the anticancer effects of EGCG without affecting normal cells. The clinical value of our findings is appreciable, because PDE5 inhibitors are widely used drugs approved by the FDA for chronic use (36). Hepatotoxicity is the well-known adverse effect of high-dose EGCG (37), and, in some cases, elevation of transaminases ALT/AST has been observed in clinical trials (13). Importantly, EGCG and vardenafil in combination did not increase the serum levels of ALT/AST.

Interestingly, there was a correlation between the expression of PDE5 and that of 67LR. However, PDE5 knockdown did not affect the expression level of 67LR. Tumor necrosis factor–α and oxidative stress have been shown to regulate PDE5 expression (38, 39). Further investigation is required to determine the molecular mechanisms of PDE5 upregulation in tumor cells.

The anticancer effects of EGCG have been shown in various types of cancer by several mechanisms. Some studies have reported the inhibitory effects of EGCG on receptor tyrosine kinase signaling pathways by disruption of the lipid order (40) or by direct binding to its ATP binding site (41). EGCG has also been demonstrated to inhibit the enzyme activities of MMPs (42), the essential enzymes for the progression and metastasis of cancer. However, these mechanisms have not been confirmed in in vivo studies (12). Here, we showed that the 67LR/cGMP pathway has a crucial role in the anticancer effect of EGCG in vivo.

From a mechanistic perspective, our finding of PDE5 overexpression in cancer cells was one reason why higher EGCG concentrations were needed to induce apoptosis, even though the dissociation constant of EGCG to 67LR is 0.04 μM (17). The difficulty in the clinical use of EGCG is due to its poor bioavailability. We found that the PDE5 inhibitor vardenafil sensitized MM cells to a methylated EGCG derivative that has been known to enhance pharmacokinetic characteristics compared with EGCG in plasma (43). Various types of EGCG derivatives can be produced by solid-phase synthesis (44). Appropriate EGCG derivatives may improve the pharmacokinetic characteristics as activators of 67LR.

In conclusion, we demonstrated that combining EGCG as a cancer-selective inducer of cGMP with a PDE5 inhibitor could be used clinically without indiscriminately affecting normal cells, thereby resulting in less toxicity and better tolerability.

Methods

Patient samples. Primary MM cells were isolated from bone marrow aspirate samples obtained from MM patients. The purity of the plasma cells (80%) was confirmed by monitoring the cell surface expression of CD138. Mononuclear cells were also obtained from peripheral blood donated by healthy volunteers. Cell lines were cultured in RPMI 1640 medium supplemented with 10% FBS. NHDFs and HUVECs were provided by Takara and maintained in RPMI 1640 with 10% FBS.

Vectors and transfections. pLKO.1-based lentiviral vectors expressing nontargeting control shRNA and shRNAs targeting eNOS, PDE5, and ASM were purchased from Sigma-Aldrich. For production of the lentivirus, a lentiviral expression vector was cotransfected with packaging vectors into lenti 293T cells as described by the manufacturer.

In vitro cell proliferation and apoptosis assays. Cells were inoculated into 24-well plates (5×10^4 cells/well) and then treated with drugs at various concentrations. The number of cells was determined by trypan-blue exclusion. Annexin V^+ MM cells were detected using the annexin V–Alexa Fluor 488 Apoptosis Detection Kit (Invitrogen). Cells were mixed with annexin V–Alexa Fluor 488 and media binding reagent. A portion of the cell suspension was then placed onto a glass slide. All images were acquired with a confocal laser microscope (A1; Nikon) and fluorescence microscope (BZ-8100; Keyence). For flow cytometric analyses, cells were double stained with annexin V–Alexa Fluor 488 and PI (Sigma-Aldrich). The percentages of annexin V^+ cells were calculated by combining annexin V^+/PI^- (early annexin V–positive) and annexin V^+/PI^+ (late annexin V–positive), followed by analyses on a FACSCalibur system (BD).

Caspase activation was measured using the CaspGLOW Fluorescein Caspase Staining Kit according to the manufacturer's protocol (Biovision). Briefly, cells were stained with the caspase family inhibitor FITC-conjugated VAD-FMK for 1 hour at 37°C in 5% CO_2. All experiments were repeated thrice, and quantitative results were analyzed by Tukey test. A *P* value less than 0.05 was considered significant.

cGMP assays. Measurements of cGMP were carried out using the AlphaScreen cGMP assay kit (Perkin-Elmer). The assays were done using the conditions described by the manufacturer. Cells were treated with reagents for 3 hours in 96-well plates. Plates were read using the EnVision Plate Reader (Perkin-Elmer) at an excitation wavelength of 680 nm and emission wavelength of 615 nm.

NO assays. Production of NO in cultured cells was assayed using the fluorescent probe 4,5-diaminofluorescein diacetate (DAF-2DA; Sekisui Medical). Cells were incubated in 10 μM DAF-2DA after the addition of EGCG. Green fluorescence of the dye was analyzed using the EnVision Plate Reader at an excitation wavelength of 460 nm and emission wavelength of 535 nm.

Western blot analyses and immunofluorescent staining. Cells were lysed in the above-mentioned lysis buffer containing 50 mM Tris-HCl (pH 7.5), 150 mM NaCl, 1% Triton X-100, 1 mM EDTA, 50 mM NaF, 30 mM $Na_4P_2O_7$, 1 mM phenylmethanesulfonyl fluoride, 2 mg/ml aprotinin, and 1 mM pervanadate. Approximately 50 μg protein was suspended in Laemmli sample buffer (0.1 M Tris-HCl buffer, pH 6.8; 1% SDS; 0.05% mercaptoethanol; 10% glycerol; and 0.001% bromophenol blue), boiled, and electrophoresed on SDS-polyacrylamide gels. Gels were then electroblotted onto Trans-Blot nitrocellulose membranes (Bio-Rad). Incubation with the indicated antibodies was done in Tween 20-PBS (TPBS) containing 1% BSA. Blots were washed with TPBS and incubated in anti-rabbit or anti-mouse HRP conjugates. After washing, specific proteins were detected using an enhanced chemiluminescence system according to the manual from Amersham Life Sciences. Patient tissue samples were purchased from US Biomax. Samples were incubated overnight at 4°C with the primary antibody. Anti-PDE5 antibodies (Abcam) were used at 1:200 dilution. Slides were then treated with Alexa Fluor 555–conjugated secondary antibody (Invitrogen) at 1:100 dilution and incubated for 1 hour. Anti-67LR Alexa Fluor 488–conjugated antibody was produced following the

manufacturer's protocol, and slides were treated with Alexa Fluor 488–conjugated anti-67LR (5 μg/ml).

Measurement of ASM activity. Cells were lysed in lysis buffer and incubated at 4°C for 1 hour, followed by centrifugation at 15,000 *g* for 15 minutes. The supernatant was incubated at 37°C for 18 hours with substrate buffer (400 pmol BODIPY-C12 sphingomyelin, 1% Triton X-100, and 200 mM sodium acetate in dH_2O).

Xenograft murine model. 5-week-old female BALB/c mice were obtained from Kyudo. Mice were inoculated subcutaneously in the interscapular area with 5×10^6 MPC-11 cells. After the appearance of palpable tumors, mice were divided randomly into groups with an even distribution of tumor sizes. They were then injected i.p. daily with saline alone, or EGCG (15 mg/kg) or vardenafil (5 mg/kg), every 2 days. 5-week-old female BALB nu/CrlCrlj mice, obtained from Charles River Laboratories, were inoculated with 5×10^6 MDA-MB-231 RFP cells, and the injection regimens described above were followed (*n* = 8 per group). Tumor growth was measured with calipers, and the tumor volume was calculated as $l \times w^2/2$. In vivo images were obtained using the Maestro II imaging system (CRI).

Statistics. All data are presented as mean ± SEM. Significance of differences between experimental variables was determined by Tukey test. Statistical analyses were undertaken using the KyPlot software program and SPSS. The level of interaction between EGCG and vardenafil was assessed by isobologram analyses using Calcusyn 2.0 software (Biosoft). Statistical analyses of survival curves were carried out using log-rank analyses of Kaplan-Meier curves. Spearman rank test was used for correlations. A *P* value less than 0.05 was considered significant.

Study approval. Studies with human samples were approved by the Ethics Committee of Faculty of Agriculture, Kyushu University. Informed consent from all patients and healthy volunteers was obtained in accordance with the Declaration of Helsinki. All animal studies were done in accordance with the law (protocol no. 105) and notification (protocol no. 6) of the Japanese government for the welfare of experimental animals. All procedures were approved by the Animal Care and Use Committee of Kyushu University and undertaken in strict accordance with institutional guidelines for handling laboratory animals.

Address correspondence to: Hirofumi Tachibana, 6-10-1 Hakozaki, Higashi-ku, Fukuoka 812-8581, Japan. Phone: 81.92.642.3008; Fax: 81.92.642.3008; E-mail: tatibana@agr.kyushu-u.ac.jp.

1. Carroll M, et al. CGP 57148, a tyrosine kinase inhibitor, inhibits the growth of cells expressing BCR-ABL, TEL-ABL, and TEL-PDGFR fusion proteins. *Blood.* 1997;90(12):4947–4952.
2. Goldenberg MM. Trastuzumab, a recombinant DNA-derived humanized monoclonal antibody, a novel agent for the treatment of metastatic breast cancer. *Clin Ther.* 1999;21(2):309–318.
3. de Thé H, Lavau C, Marchio A, Chomienne C, Degos L, Dejean A. The PML-RAR alpha fusion mRNA generated by the t(15;17) translocation in acute promyelocytic leukemia encodes a function-

ally altered RAR. *Cell.* 1991;66(4):675–684.
4. Li D, et al. 67-kDa laminin receptor in human bile duct carcinoma. *Eur Surg Res.* 2009;42(3):168–173.
5. Sanjuan X, et al. Overexpression of the 67-kD laminin receptor correlates with tumor progression in human colorectal carcinoma. *J Pathol.* 1996; 179(4):376–380.
6. al-Saleh W, Delvenne P, van den Brule FA, Menard S, Boniver J, Castronovo V. Expression of the 67 KD laminin receptor in human cervical preneoplastic and neoplastic squamous epithelial lesions: an immunohistochemical study. *J Pathol.*

1997;181(3):287–293.
7. Viacava P, Naccarato AG, Collecchi P, Ménard S, Castronovo V, Bevilacqua G. The spectrum of 67-kD laminin receptor expression in breast carcinoma progression. *J Pathol.* 1997;182(1):36–44.
8. Scheiman J, Tseng JC, Zheng Y, Meruelo D. Multiple functions of the 37/67-kd laminin receptor make it a suitable target for novel cancer gene therapy. *Mol Ther.* 2009;18(1):63–74.
9. Liu L, et al. Hypoxia-mediated up-regulation of MGr1-Ag/37LRP in gastric cancers occurs via hypoxia-inducible-factor 1-dependent mechanism

and contributes to drug resistance. *J Int Cancer*. 2009; 124(7):1707–1715.

10. Chen ZP, Schell JB, Ho CT, Chen KY. Green tea epigallocatechin gallate shows a pronounced growth inhibitory effect on cancerous cells but not on their normal counterparts. *Cancer Lett*. 1998; 129(2):173–179.

11. Shammas MA, et al. Specific killing of multiple myeloma cells by (–)-epigallocatechin-3-gallate extracted from green tea: biologic activity and therapeutic implications. *Blood*. 2006;108(8):2804–2810.

12. Yang CS, Wang X, Lu G, Picinich SC. Cancer prevention by tea: animal studies, molecular mechanisms and human relevance. *Nat Rev*. 2009; 9(6):429–439.

13. Shanafelt TD, et al. Phase I trial of daily oral polyphenon E in patients with asymptomatic Rai stage 0 to II chronic lymphocytic leukemia. *J Clin Oncol*. 2009; 27(23):3808–3814.

14. Bettuzzi S, et al. Chemoprevention of human prostate cancer by oral administration of green tea catechins in volunteers with high-grade prostate intraepithelial neoplasia: a preliminary report from a one-year proof-of-principle study. *Cancer Res*. 2006;66(2):1234–1240.

15. McLarty J, Bigelow RL, Smith M, Elmajian D, Ankem M, Cardelli JA. Tea polyphenols decrease serum levels of prostate-specific antigen, hepatocyte growth factor, and vascular endothelial growth factor in prostate cancer patients and inhibit production of hepatocyte growth factor and vascular endothelial growth factor in vitro. *Cancer Prev Res*. 2009;2(7):673–682.

16. Brausi M, Rizzi F, Bettuzzi S. Chemoprevention of human prostate cancer by green tea catechins: two years later. A follow-up update. *Eur Urol*. 2008; 54(2):472–473.

17. Tachibana H, Koga K, Fujimura Y, Yamada K. A receptor for green tea polyphenol EGCG. *Nat Struct Mol Biol*. 2004;11(4):380–381.

18. Umeda D, Yano S, Yamada K, Tachibana H. Green tea polyphenol epigallocatechin-3-gallate signaling pathway through 67-kDa laminin receptor. *J Biol Chem*. 2008;283(6):3050–3058.

19. Lugnier C. Cyclic nucleotide phosphodiesterase (PDE) superfamily: a new target for the development of specific therapeutic agents. *Pharmacol Ther*. 2009; 109(3):366–398.

20. Keravis T, Lugnier C. Cyclic nucleotide phosphodiesterase (PDE) isozymes as targets of the intracellular signalling network: benefits of PDE inhibitors in various diseases and perspectives for future therapeutic developments. *Br J Pharmacol*. 2012;165(5):1288–1305.

21. Porst H, et al. The efficacy and tolerability of vardenafil, a new, oral, selective phosphodiesterase type 5 inhibitor, in patients with erectile dysfunction: the first at-home clinical trial. *Int J Impotence Res*. 2001; 13(4):192–199.

22. Gloe T, Riedmayr S, Sohn HY, Pohl U. The 67-kDa laminin-binding protein is involved in shear stress-dependent endothelial NO synthase expression. *J Biol Chem*. 1999;274(23):15996–16002.

23. Dimmeler S, Fleming I, Fisslthaler B, Hermann C, Busse R, Zeiher AM. Activation of nitric oxide synthase in endothelial cells by Akt-dependent phosphorylation. *Nature*. 1999;399(6736):601–605.

24. Arnold WP, Mittal CK, Katsuki S, Murad F. Nitric oxide activates guanylate cyclase and increases guanosine 3′:5′-cyclic monophosphate levels in various tissue preparations. *Proc Natl Acad Sci U S A*. 1977; 74(8):3203–3207.

25. Tsukamoto S, et al. Green tea polyphenol EGCG induces lipid raft clustering and apoptotic cell death by activating protein kinase Cδ and acid sphingomyelinase through 67-kDa laminin receptor in multiple myeloma cells. *Biochem J*. 2012; 443(2):525–534.

26. Gou S, et al. Establishment of clonal colony-forming assay for propagation of pancreatic cancer cells with stem cell properties. *Pancreas*. 2007;34(4):429–435.

27. Wen J, et al. A2B adenosine receptor contributes to penile erection via PI3K/AKT signaling cascade-mediated eNOS activation. *FASEB J*. 2011; 25(8):2823–2830.

28. Efimova T, Eckert RL. Regulation of human involucrin promoter activity by novel protein kinase C isoforms. *J Biol Chem*. 2000;275(3):1601–1607.

29. Hung JH, et al. FTY720 induces apoptosis in hepatocellular carcinoma cells through activation of protein kinase Cδ signaling. *Cancer Res*. 2008; 68(4):1204–1212.

30. Blass M, et al. Tyrosine phosphorylation of protein kinase C δ is essential for its apoptotic effect in response to etoposide. *Mol Cell Biol*. 2002; 22(1):182–195.

31. Cataldi A, Di GV, Rapino M, Zara S, Rana RA. Ionizing radiation induces apoptotic signal through protein kinase C delta and survival signal through Akt and cyclic-nucleotide response element-binding protein (CREB) in Jurkat T cells. *Biol Bull*. 2009; 217(2):202–212.

32. Mizuno K, et al. The proteolytic cleavage of protein kinase C isotypes, which generates kinase and regulatory fragments, correlates with Fas-mediated and 12-O-tetradecanoyl-phorbol-13-acetate-induced apoptosis. *Eur J Biochem*. 1997;250(1):7–18.

33. Zhang S, et al. Combating trastuzumab resistance by targeting SRC, a common node downstream of multiple resistance pathways. *Nat Med*. 2011; 17(4):461–469.

34. Ito K, et al. PML targeting eradicates quiescent leukaemia-initiating cells. *Nature*. 2008; 453(7198):1072–1078.

35. Dai B, et al. Functional and molecular interactions between ERK and CHK2 in diffuse large B-cell lymphoma. *Nat Commun*. 2011;2:402.

36. Jaumann M, et al. cGMP-Prkg1 signaling and Pde5 inhibition shelter cochlear hair cells and hearing function. *Nat Med*. 2012;18(2):252–259.

37. Lambert JD, Kennett MJ, Sang S, Reuhl KR, Ju J, Yang CS. Hepatotoxicity of high oral dose (–)-epigallocatechin-3-gallate in mice. *Food Chem Toxicol*. 2010; 48(1):409–416.

38. Hotston MR, et al. Homocysteine and copper interact to promote type 5 phosphodiesterase expression in rabbit cavernosal smooth muscle cells. *Asian J Androl*. 2008;10(6):905–913.

39. Hotston MR, et al. Sildenafil inhibits the up-regulation of phosphodiesterase type 5 elicited with nicotine and tumour necrosis factor-alpha in cavernosal vascular smooth muscle cells: mediation by superoxide. *BJU Int*. 2007;99(3):612–618.

40. Adachi S, et al. The inhibitory effect of (–)-epigallocatechin gallate on activation of the epidermal growth factor receptor is associated with altered lipid order in HT29 colon cancer cells. *Cancer Res*. 2007;67(13):6493–6501.

41. Li M, et al. Direct inhibition of insulin-like growth factor-I receptor kinase activity by (–)-epigallocatechin-3-gallate regulates cell transformation. *Cancer Epidemiol Biomarkers Prev*. 2007;16(3):598–605.

42. Garbisa S, et al. Tumor gelatinases and invasion inhibited by the green tea flavanol epigallocatechin-3-gallate. *Cancer*. 2001;91(4):822–832.

43. Maeda-Yamamoto M, Ema K, Shibuichi I. In vitro and in vivo anti-allergic effects of 'benifuuki' green tea containing O-methylated catechin and ginger extract enhancement. *Cytotechnology*. 2007; 55(2–3):135–142.

44. Tanaka H, Yamanouchi M, Miyoshi H, Hirotsu K, Tachibana H, Takahashi T. Solid-phase synthesis of a combinatorial methylated (±)-epigallocatechin gallate library and the growth-inhibitory effects of these compounds on melanoma B16 cells. *Chem Asian J*. 2010;5(10):2231–2248.